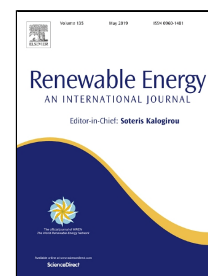


Accepted Manuscript

Investigation of solid base catalysts for biodiesel production from fish oil

Despoina Papargyriou, Emmanouil Broumidis, Matthew de Vere-Tucker, Stelios Gavrielides, Paul Hilditch, John T.S. Irvine, Alfredo D. Bonaccorso



PII: S0960-1481(19)30289-7
DOI: 10.1016/j.renene.2019.02.124
Reference: RENE 11256
To appear in: *Renewable Energy*
Received Date: 04 December 2018
Accepted Date: 22 February 2019

Please cite this article as: Despoina Papargyriou, Emmanouil Broumidis, Matthew de Vere-Tucker, Stelios Gavrielides, Paul Hilditch, John T.S. Irvine, Alfredo D. Bonaccorso, Investigation of solid base catalysts for biodiesel production from fish oil, *Renewable Energy* (2019), doi: 10.1016/j.renene.2019.02.124

This is a PDF file of an unedited manuscript that has been accepted for publication. As a service to our customers we are providing this early version of the manuscript. The manuscript will undergo copyediting, typesetting, and review of the resulting proof before it is published in its final form. Please note that during the production process errors may be discovered which could affect the content, and all legal disclaimers that apply to the journal pertain.

Investigation of solid base catalysts for biodiesel production from fish oil

Despoina Papargyriou ¹, Emmanouil Broumidis ¹, Matthew de Vere-Tucker ¹, Stelios Gavrielides ¹, Paul Hilditch ², John T. S. Irvine ¹, Alfredo D. Bonaccorso ¹

¹School of Chemistry, University of St Andrews, North Haugh, St Andrews, KY16 9ST, UK

²Green Fuels Research, B21 Gloucestershire Science & Technology Park, Berkeley, GL13 9FB, UK

Abstract

A series of composite CaO-Ca₃Al₂O₆ mixed oxides were investigated as potential catalysts for biodiesel synthesis from waste fish oil. Different Ca/Al ratios, in the range of 1.5 to 6 were studied, alongside pure CaO. The catalysts were characterised by X-ray diffraction (XRD), scanning electron microscopy (SEM) and CO₂-Temperature Program Desorption (TPD). The catalytic activity of the materials was studied for the transesterification reaction of cod liver oil with methanol at 65 °C, with 1:12 oil to methanol molar ratio and 10 wt% of catalyst. Over 97% conversion of the triglycerides to methyl esters was achieved for the 6Ca/Al catalyst after 2 h reaction time. This was similar to the performance of CaO. However, 6Ca/Al catalyst was reused successfully for seven consecutive tests, in contrast to CaO that was reused for only five tests, before it deactivated. Therefore, by incorporating the Ca₃Al₂O₆, it was possible to enhance the stability of the catalytically active species and improve the lifetime of the catalyst. Post-test catalyst characterisation showed the formation of an intermediate phase (calcium diglyceroxide) that enhanced the catalyst's performance and tolerance to air exposure and humidity. Finally, the catalyst deactivation, after seven cycles, took place due to the formation of Ca(OH)₂ and CaCO₃ species.

Keywords: biodiesel, heterogeneous catalyst, waste fish oil, transesterification reaction

1. Introduction

The aquaculture industry produces large amounts of waste which has low commercial value. This waste is produced during food processing, where the main product is the fillet of the fish, which represents only 30% of the wet fish weight and the rest is discarded.[1] This waste has been typically used in animal feed or fertilisers.[1–3] However, there is a significant opportunity to utilise this for the production of renewable fuel. More specifically, as the fish waste that comes from the food processing has high oil content, it is possible to use it as feedstock for the production of biodiesel.[1,4–6] Fish oil extracted from waste not only reduces the amount of waste that is generated, but also reduces the

34 total cost of biodiesel synthesis.[3] Moreover, this biodiesel can be used by the local farmers in the
35 diesel generators or sold for blending with mineral diesel, allowing them to be energy independent,
36 while reducing their waste disposal burden. Therefore, there is a great opportunity to produce low cost
37 biodiesel from fish waste, produced by an important agricultural industry.

38 Biodiesel is a biodegradable fuel that is produced from plant- or animal- derived oils or fats. It is
39 comprised of fatty acid alkyl esters, obtained during the transesterification reaction of triglycerides of
40 lipids with low molecular weight alcohols.[7–10] Biodiesel is non-toxic and a cleaner-burning fuel than
41 fossil diesel. It has no aromatics and a higher flash point than petrodiesel.[11] Some of the technical
42 challenges associated with the use of biodiesel are its low oxidation stability, poor cold flow properties
43 and low energy content.[12] These properties are mainly dependent on the fatty acid profile of the
44 biodiesel, which corresponds to that of the feedstock it is obtained from.[11] However, since biodiesel
45 is miscible with fossil diesel, it can be blended in different ratios with it. As a result, the fuel properties
46 can be improved, and it can be used in the existing fuel distribution infrastructure.[11,12]

47 The transesterification reaction for biodiesel synthesis can be catalysed by both acids and bases, with
48 base catalysis being considerably more rapid.[11] Traditionally, the biodiesel synthesis takes place in
49 moderate reaction conditions (60 °C, 1 atm), in the presence of alkaline homogeneous catalysts such
50 as sodium methoxide and sodium or potassium hydroxide.[11] Although these catalysts demonstrate
51 fast reaction rates, they contaminate the biodiesel and extra separation and purification steps are
52 required, increasing the cost and energy requirements of the production.^{9–12} Therefore, different
53 approaches have been investigated to improve the process efficiency for the biodiesel production.

54 Many studies have focused on improving the heat and mass transfer limitations that take place due to
55 the immiscibility of the oil and methanol phases. The implementation of novel reactor designs,[16–18]
56 the operation at supercritical conditions,[19] the addition of co-solvents[20] and the use of
57 ultrasounds[21] or microwaves[22] have shown promising results. Other approaches have focused on
58 reducing the cost of the separation and purification of the product by performing simultaneous reaction
59 and separation. This was achieved by using membrane reactors[23] or reactive distillation.[24] Finally,
60 a lot of research has been conducted on performing the transesterification reaction heterogeneously,
61 adding an enzymatic or inorganic solid base catalyst.[8] However, enzymatic catalysts are less
62 attractive than the inorganic, due to their high synthesis cost and longer reaction times.[25]

63 The use of inorganic solid base catalysts offers many benefits for the biodiesel production. These
64 catalysts can be easily separated from the reaction mixture and recycled.[11] As a result, the biodiesel
65 production is more economically feasible and environmentally friendly.[15] In addition to that, the
66 separation of the glycerol from the biodiesel is much simpler and no purification step is required.
67 Moreover, these catalysts can be used in a continuous process, which can further reduce the capital
68 cost of the biodiesel synthesis.[26]

69 Diverse solid base catalysts have been investigated for this purpose. Scientists have studied alkaline
70 earth oxides, such as CaO, MgO and SrO.[10] These catalysts demonstrate strong basic sites, which
71 are beneficial to the transesterification reaction and show high catalytic activity.[27] Doping the alkaline
72 earth oxides with alkali metals can enhance their basicity and consequently their catalytic activity. For
73 instance, the Li-doped CaO catalysts demonstrated enhanced catalytic activity, but the leaching of the
74 alkali promoters was problematic during repeated cycling.[28] To increase the recyclability of the
75 heterogeneous catalysts, the incorporation of the active phase on a support has been investigated.[26]
76 Typical examples are CaO supported on Al₂O₃[29,30] and KF/Ca–Al hydrotalcites.[31] Finally, the
77 hydrotalcites demonstrate high intrinsic activity for the transesterification reaction of lipids,[32] but they
78 are poorly suited for bulky C16-C18 triglycerides, due to their low surface area.[33]

79 The CaO-based materials are some of the most promising heterogeneous catalysts for biodiesel
80 production from vegetable oils or animal fats.[34–36] These catalysts are low-cost materials, with high
81 basicity and demonstrate high activity in moderate reaction conditions. However, one of the main
82 limitations of these catalysts is the deactivation during repeated tests, due to leaching of Ca²⁺ ions,
83 which also leads to contamination of the biodiesel.[27] One approach to overcome this issue is to use
84 mixtures of CaO with other metal oxides, which can enhance both the catalysts stability and catalytic
85 activity. Typical examples are studies on CaO and ZrO₂ mixed catalysts,[37] CaO supported on La₂O₃
86 and CeO₂[38] or composite oxide containing CaO and Ca₁₂Al₁₄O₃₃.[39,40]

87 In this work, the synthesis and characterisation of a series of catalysts, comprising CaO and Ca₃Al₂O₆,
88 are investigated for biodiesel production from waste fish oil. Finally, the catalytic activity and reusability
89 of these catalysts are evaluated with cod liver oil, to determine the optimum catalyst in terms of
90 performance and stability for biodiesel production from waste fish oil.

91 **2. Experimental**

92 **2.1. Synthesis of the catalysts**

93 The catalysts were prepared by combustion synthesis with ethylene glycol and citric acid. Appropriate
94 stoichiometric ratios of Ca(NO₃)₂·4H₂O and Al(NO₃)₃·9H₂O were diluted in deionised water, with
95 ethylene glycol and citric acid. The solution was heated under stirring at 100 °C to evaporate the water
96 and it was then combusted at 300 °C. The resulting powder was calcined at 1000 °C for 5 h and a
97 mixed oxide phase of CaO and Ca₃Al₂O₆ (C3A) was obtained. Different Ca/Al ratios were investigated
98 in the range of 1.5 to 6, which resulted to different CaO/C3A ratios. Moreover, commercial CaO powder
99 was used as reference. The compositions of the catalysts synthesised in this work and their
100 abbreviations are summarised in Table 1.

101

102

103 Table 1 Composition of the synthesised catalysts and their abbreviations

| Catalyst abbreviation | Ca/Al molar ratio | CaO (wt.%) * | C3A (wt.%) * |
|-----------------------|-------------------|--------------|--------------|
| CaO | - | 100 | 0 |
| 6Ca/Al | 6 | 65 | 35 |
| 3Ca/Al | 3 | 38 | 62 |
| 2Ca/Al | 2 | 17 | 83 |
| C3A | 1.5 | 0 | 100 |

* Theoretical values

104 **2.2. Characterisation techniques**

105 Room temperature powder X-ray diffraction (XRD) was performed on a PANalytical Empyrean
 106 diffractometer operated in reflection mode using Cu-K α 1 radiation. The obtained XRD patterns were
 107 analysed with STOE Win XPOW software to determine the crystal structure of the catalysts and the
 108 evolution of different phases during testing. The microstructure of the samples was analysed with a
 109 JEOL JSM-6700 field emission scanning electron microscope (FEG-SEM). Elemental analysis was
 110 performed with an Oxford Inca EDX system. Fourier-transform infrared (FTIR) spectra were recorded
 111 using a Shimadzu IRAffinity 1S IR spectrometer. Measurements were conducted in wavenumber
 112 range of 4000–600 cm⁻¹. The Ca/Al ratio of the catalysts was determined by inductively coupled
 113 plasma optical emission spectroscopy (ICP-OES) on a Thermo-iCAP 6000 spectrometer. The samples
 114 were treated in hydrochloric acid and compared to standards.

115 The total basicity of the prepared catalysts was measured based on their temperature programmed
 116 CO₂ desorption profiles. The catalysts were pre-treated at 800 °C under an Ar flow rate of 50 ml/min
 117 to remove any adsorbed CO₂ and water from their surface and then cooled down to 50 °C. At this
 118 temperature, the CO₂ chemisorption was carried out in a CO₂ flow rate of 50 ml/min for 2 h. The excess
 119 of CO₂ was then desorbed at the temperature of the adsorption in an Ar flow (50 ml/min) for 2 h.
 120 Finally, desorption of CO₂ took place with Ar from 100 to 800 °C. The evolution of the mass of the
 121 catalysts during these treatments was measured using Thermogravimetric analysis (TGA) in a
 122 Netzsch STA 449C instrument. The TGA was equipped with a Pfeiffer mass spectrometer (MS), which
 123 analysed the CO₂ evolution during the different steps.

124 **2.3. Physicochemical characterisation of the fish oil**

125 The evaluation of the catalysts' activity for the transesterification reaction was performed with
 126 commercial cod liver oil, purchased from Holland and Barrette, UK. Fish oil methyl esters were

127 analysed with a GC-MS (Agilent, Intuvo 9000 GC), equipped with an Agilent DB-23 column. The free
 128 fatty acid composition of the fish oil is presented in Table 2. It consists mainly of palmitic acid (14.2%),
 129 oleic acid (13.8%), palmitoleic acid (11.7%), docosahexaenoic acid (11.2%), eicosapentaenoic acid
 130 (9.6%) and cis-11-eicosenoic acid (9.1%).

131 Table 2 Free fatty acid % composition of the cod liver oil

| Free Fatty Acids | Lipid Number | Composition (%) |
|-------------------------|--------------|-----------------|
| Myristic acid | C14 | 8.9 |
| Palmitic acid | C16 | 14.2 |
| Palmitoleic acid | C16:1 | 11.7 |
| Stearic acid | C18 | 5.8 |
| Oleic acid | C18:1 | 13.8 |
| Linoleic acid | C18:2 | 3.4 |
| α -Linoleic acid | C18:3 | 1.7 |
| Stearidonic acid | C18:4 | 4.3 |
| cis-11-eicosenoic acid | C20:1 | 9.1 |
| Eicosapentaenoic acid | C20:5 | 9.6 |
| Erucic acid | C22:1 | 6.3 |
| Docosahexaenoic acid | C22:6 | 11.2 |

132

133 The physicochemical properties of the fish oil are summarised in Table 3. The cod liver oil was yellow
 134 in colour with typical smell. The density of the oil was 897 kg/m³ and the boiling point was 420 °C. No
 135 impurities or water were present in the fish oil and the acid value was 0.53 mg KOH/g. Therefore, this
 136 was a suitable feedstock to perform the transesterification reaction with the synthesised catalysts for
 137 biodiesel synthesis.

138

139

140

141 Table 3 Physicochemical properties of the cod liver oil

| Property | Value |
|------------------------------|-----------------------|
| Visual observations at 15 °C | Yellow liquid |
| Density at 15 °C | 897 kg/m ³ |
| Boiling point | 420 °C |
| Water content | <0.001 wt.% |
| Acid value | 0.53 mg KOH/g |

142

143 **2.4. The transesterification reaction**

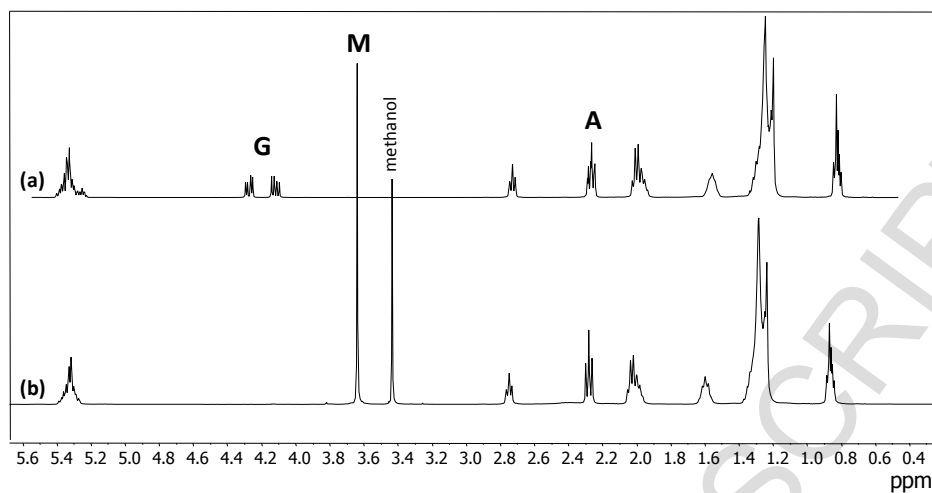
144 The transesterification was performed in a 100 ml three-neck round-bottom flask equipped with a
145 water-cooled reflux condenser and a magnetic stirrer. The temperature was controlled at 65 °C with
146 an oil bath and it was monitored during the reaction with a thermocouple probe that was placed in the
147 reaction mixture. Appropriate amounts of fish oil, methanol and catalyst were used based on the
148 requirements of each experiment and the reaction mixture was stirred at 800 rpm to achieve uniform
149 temperature distribution and suspension of the catalyst in the reaction mixture. Samples from the
150 reaction mixture were collected in different time intervals, for monitoring the evolution of the
151 transesterification reaction. After running the reaction for the desirable duration, the mixture was
152 centrifuged at 1400 rpm, the liquid was decanted, and the remaining catalyst was filtered under
153 vacuum and washed thoroughly with methanol. Then, the recovered catalyst was dried in the oven
154 (80 °C) overnight and it was used for analysis and recyclability tests. No fresh catalyst was added
155 during the catalysts recycling. The reaction was carried out with an oil to methanol ratio of 1 to 12,
156 catalyst loading of 10 wt.% based on the fish oil weight and reaction times of up to 4 h.

157 The conversion of the fish oil triglycerides to the methyl esters of the biodiesel was determined by H¹
158 Nuclear Magnetic Resonance (NMR) in a Bruker AVII 400 spectrometer. Figure 1 presents the H¹
159 NMR spectra of cod liver oil and of the biodiesel produced, when full conversion of the triglycerides
160 (G) to methyl esters (M) took place. The conversion was calculated based on the integration of the
161 signal at 3.68 ppm (M) and at 2.30 ppm (A), according to equation (1).[41] The signal at 3.68 ppm
162 corresponds to the hydrogen of the methoxy groups in the methyl esters and at 2.30 ppm to the
163 hydrogen of the methylene groups of the fatty acid derivatives. Finally, the signals between 4.3-4.1
164 belong to the glyceride protons and therefore they disappear when full conversion of the fish oil to
165 biodiesel takes place.

166

$$C_{ME} = \frac{2 \cdot I_M}{3 \cdot I_A} \quad (1)$$

167



168

169 Figure 1 ^1H NMR spectra of a) cod liver oil and b) biodiesel produced after the transesterification reaction of the
 170 fish oil

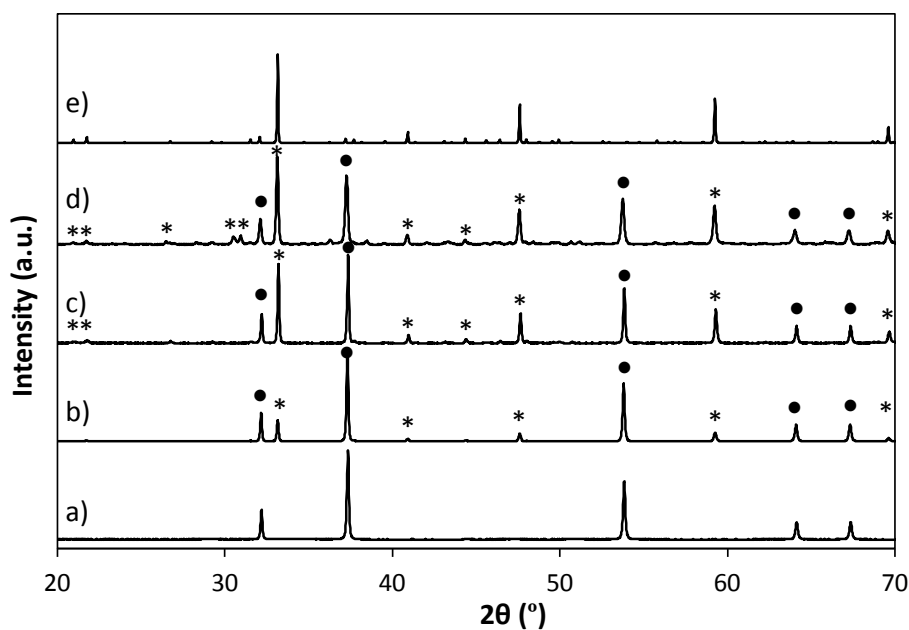
171

172 3. Results and discussion

173 3.1. XRD analysis of the synthesised catalysts

174 The XRD patterns of the synthesised catalysts with the different Ca/Al molar ratios are presented in
 175 Figure 2. For a Ca/Al ratio of 1.5, a single phase C3A material was obtained, with cubic structure, $Pa-3$
 176 space group and cell volume $V=3558.74(5)$ Å. By increasing the Ca/Al ratio up to 6, a mixed phase of
 177 C3A and CaO was obtained. It is worth noting that no other intermediate phases were evident by XRD.
 178 According to Figure 2, by increasing the Ca/Al ratio there was an increase in the CaO content and a
 179 decrease in the C3A phase.

180



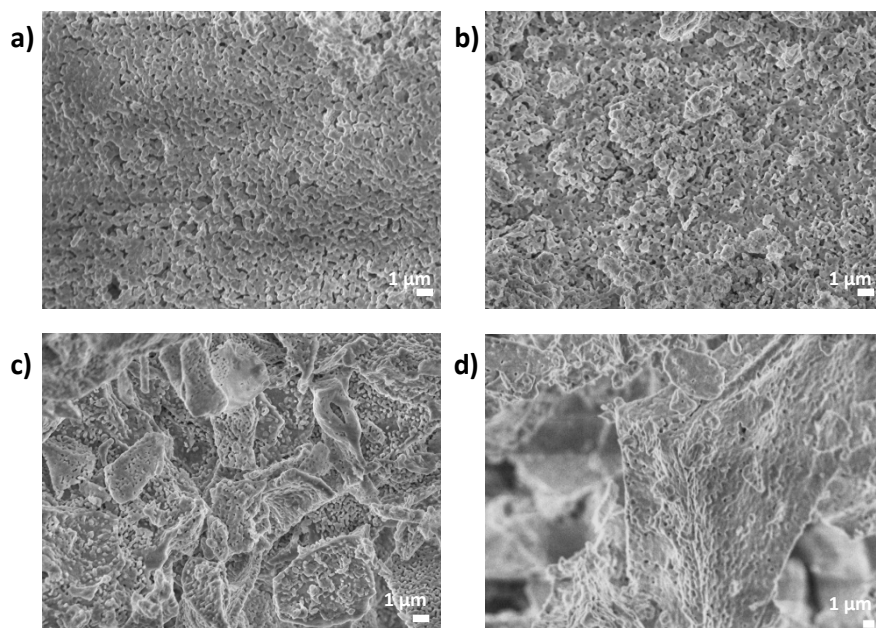
181

182 Figure 2 XRD patterns of the synthesised catalysts a) CaO, b) 6Ca/Al, c) 3Ca/Al, d) 2Ca/Al, e) C3A, where (*)
 183 corresponds to the C3A phase and (●) to the CaO phase

184

185 3.2. Catalysts microstructure

186 The microstructure of the catalysts was observed by SEM. Figure 3 illustrates the SEM micrographs
 187 of the catalysts with the different Ca/Al ratios after calcination at 1000 °C for 5 h. Based on Figure 3,
 188 it is evident that the catalyst is a two phase system, where the CaO phase presented smaller particles
 189 and the C3A phase formed larger and more agglomerated particles. By increasing the Al content, the
 190 formation of the C3A phase was more evident. Consequently, the formation of the CaO phase
 191 decreased. Moreover, for high Ca/Al ratios the particles of the catalyst comprised a uniformly
 192 dispersed mixture of CaO and C3A (Figure 3 a,b), while for lower Ca/Al ratios the particles of the CaO
 193 phase were partially coated on the C3A particles (Figure 3 c). This shows the Ca/Al ratio can influence
 194 the distribution of the two phases and the microstructure of the catalyst.



195

196 Figure 3 SEM micrographs of the CaO-C3A catalysts a) 6Ca/Al, b) 3Ca/Al, c) 2Ca/Al and d) C3A

197

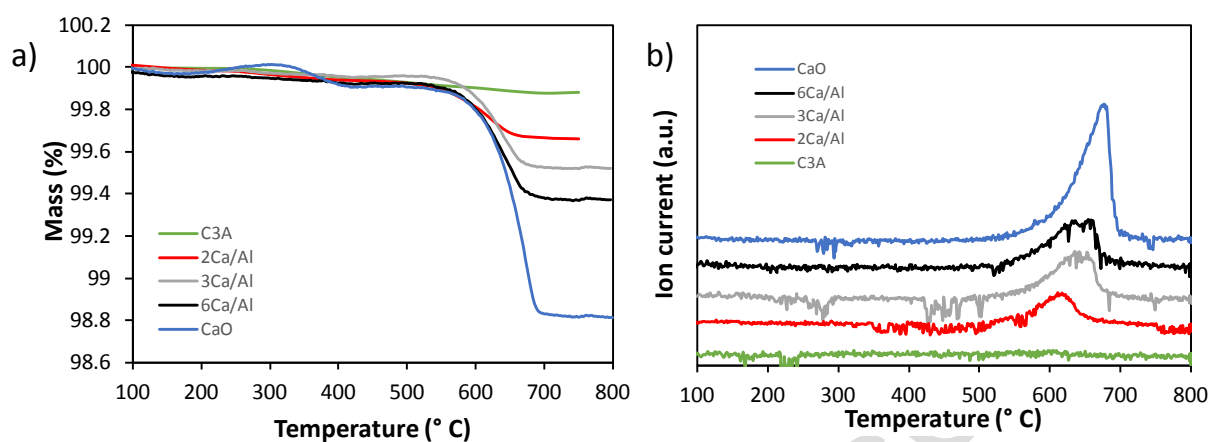
198 3.3. CO₂ desorption profiles of the catalysts

199 The basicity of the synthesised catalysts was determined from their CO₂ desorption profiles. Figure
 200 4a presents the evolution of the catalysts mass in relation to temperature during the CO₂ desorption
 201 step, as recorded by the TGA. The main weight loss occurred in one step between 600 and 700 °C
 202 and corresponds to the CO₂ desorbed on the catalyst's basic sites. The largest weight loss was
 203 observed for CaO and by decreasing the Ca/Al ratio, the amount of CO₂ desorbed by the catalyst was
 204 reduced. Finally, pure C3A with no free CaO demonstrated no weight loss, therefore no CO₂
 205 desorption took place.

206 Figure 4b shows the CO₂ gas evolution when the CO₂ desorption took place between 100 and 800 °C,
 207 as it was recorded by the MS. The temperature where the CO₂ signal was detected corresponded to
 208 the temperature where the samples lost mass, due to the CO₂ desorption from the catalysts. The
 209 strongest CO₂ signal was detected for pure CaO at approximately 670 °C and was attributed to the
 210 strong basic sites corresponding to unbonded O²⁻ anions of CaO. [31,37,42–44] Moreover, no CO₂
 211 signal was observed for pure C3A, as was expected based on the TGA results. By decreasing the
 212 Ca/Al ratio from 6 to 2, the CO₂ signal decreased and a slight shift of the desorption temperature from
 213 670 to 610 °C was observed. These results suggest that when larger Ca/Al ratios are used, the number
 214 of the basic sites increases. There is more free CaO on the catalyst and therefore the observed CO₂
 215 signal is stronger. This indicates, the CaO phase is the active species in this catalytic system and the
 216 C3A phase acts as a support and stabilises the active species. Finally, the shift of the desorption

217 temperature to lower values can be attributed to the acidic contribution of the C3A phase on the
 218 composite catalysts that reduced the basic strength of the catalyst.

219



220

221 Figure 4 CO₂ desorption profiles of the synthesised catalysts a) mass evolution with temperature b) CO₂ gas
 222 evolution with temperature

223

224 3.4. The transesterification reaction

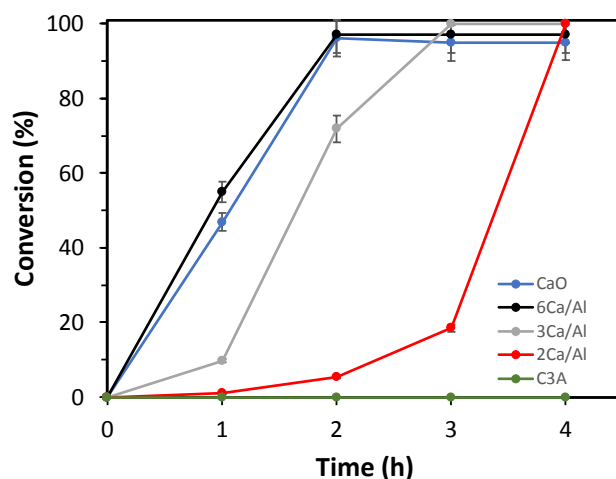
225 3.4.1. Catalysts activity

226 The catalytic activity of these samples was investigated for the transesterification reaction of cod liver
 227 oil to biodiesel. The samples were tested using the same reaction conditions to compare their catalytic
 228 activity and the influence of the Ca/Al ratio to the transesterification reaction. The reaction was carried
 229 out at 65 °C, with 1:12 oil to methanol molar ratio and a stirring speed of 800 rpm. The amount of
 230 catalyst used was fixed at 10 wt.% based on the oil used. Figure 5 presents the evolution of the
 231 conversion of the triglycerides to methyl esters with time for each catalyst. The conversion of the cod
 232 liver oil triglycerides to methyl esters in different time intervals was calculated by H¹ NMR, according
 233 to eq. 1.

234 According to Figure 5, all the catalysts demonstrated a conversion higher than 95% after a maximum
 235 of 4 h reaction time, except C3A. However, it is worth pointing out that the reaction rates differed and
 236 were proportional to the Ca/Al ratio. More specifically, no conversion was observed for C3A. The
 237 slowest reaction rate was demonstrated by 2Ca/Al and full conversion was achieved after 4 h.
 238 Following that, 3Ca/Al showed full conversion after 3 h and then 6Ca/Al after 2 h. Finally, pure CaO
 239 demonstrated full conversion after 2 h, which was similar to 6Ca/Al.

240 The differences in the catalysts' activity was related to their basicity. The more basic sites present on
 241 the catalyst, the faster the rate of reaction for biodiesel production is. This coincides with the CO₂ TPD
 242 results presented in Figure 4. As previously mentioned, C3A showed no CO₂ adsorption and therefore

243 it did not demonstrate any triglycerides conversion to biodiesel. By increasing the Ca/Al ratio of the
 244 catalyst and consequently creating more basic sites within the catalyst, the catalytic activity increased,
 245 and the transesterification reaction occurred at a faster rate. It is worth mentioning that 6Ca/Al catalyst
 246 performed with similar reaction rates as pure CaO. Thus, the stability of these two different catalytic
 247 systems was investigated, as explained in the following section.



248

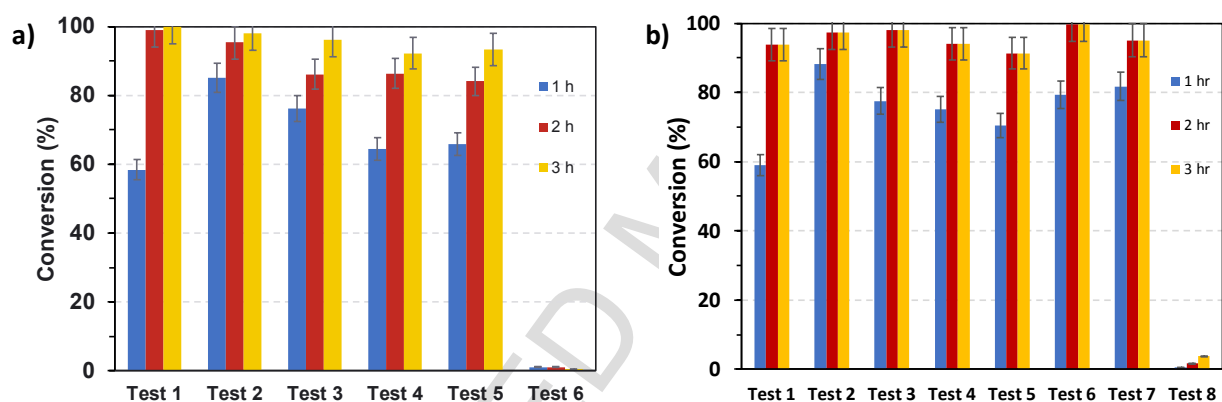
249 Figure 5 Triglycerides conversion to methyl esters over time for the synthesised catalysts

250

251 3.4.2. Catalysts recyclability

252 The reusability of the catalysts was investigated, by recovering the used catalyst and repeating the
 253 transesterification reaction with the same sample. Figure 6 presents the results from the recyclability
 254 tests of CaO and 6Ca/Al, the two samples that demonstrated similar catalytic activity and reaction
 255 rates. CaO was recycled and performed with over 95% conversion for five tests and was fully
 256 deactivated on the sixth test. However, 6Ca/Al catalyst demonstrated better stability than CaO and
 257 performed successfully for seven tests and was finally deactivated on the eighth test. An interesting
 258 observation was made regarding the changes in the reaction rates of the catalysts during the different
 259 tests performed. More specifically, CaO demonstrated roughly 60% conversion during the first hour of
 260 the first test. However, on the second test the conversion after the first hour increased to 85%. Then,
 261 the conversion in the first hour of each test gradually decreased and the catalyst was deactivated by
 262 the sixth test. Similar behaviour was observed for the 6Ca/Al catalyst, which was deactivated on test
 263 eight. This is discussed in detail in section 3.6, considering the changes in the catalysts structure.
 264 Overall, the recyclability tests showed that by incorporating the C3A phase into the catalyst, the
 265 stability of the CaO phase can be enhanced significantly, due to the interaction between the two
 266 phases.

267 According to the literature, the stability of CaO during biodiesel production is limited to approximately
 268 five cycles, if no catalyst pre-treatment is performed.[27,45] Many scientists have tried to stabilise CaO
 269 by incorporating another oxide phase. Dekhordi *et al.* have prepared CaO and ZrO₂ mixed oxides for
 270 the transesterification of waste cooking oil.[37] They found by increasing the Zr:Ca ratios the stability
 271 of the catalyst increased but the activity was dependent on the CaO content. The optimum Ca/Zr ratio
 272 was 0.5 and when they operated with 10 wt.% catalyst, 30:1 methanol to oil molar ratio and 2 h reaction
 273 time, they achieved a biodiesel yield of 92%. However, when the catalyst was recycled, the biodiesel
 274 yield decreased to 80% after 10 cycles.[37] Another interesting example is the Ca₁₂Al₁₄O₃₃ and CaO
 275 mixed oxide catalyst used for the transesterification of rapeseed oil.[39] This catalyst achieved 87%
 276 conversion over seven cycles at 65 °C, with a 15:1 methanol to rapeseed molar oil ratio, 6 wt.% of
 277 catalyst and 3 h reaction time.[39] In this work, 6Ca/Al demonstrated 97% triglycerides conversion to
 278 methyl esters, operating at 65 °C, with 10 wt.% catalyst, 12:1 methanol to oil molar ratio and 2 h
 279 reaction time. The conversion was retained above 95% for seven consecutive cycles and no catalyst
 280 pre-treatment was performed. This catalyst has demonstrated superior performance and enhanced
 281 stability for biodiesel production from cod liver oil.



282

283 Figure 6 Recyclability tests of a) CaO and b) 6Ca/Al catalysts

284

285 3.4.3. Biodiesel properties

286 The physicochemical properties of the biodiesel produced from cod liver oil with the 6Ca/Al catalyst
 287 are presented in Table 4. After the transesterification reaction, the density of the fish oil decreased
 288 from 897 kg/m³ to 888 kg/m³, the boiling point dropped from 420 to 227 °C and the ester content was
 289 97%. These physicochemical properties meet the EU standard limits. Only the acid value of the fish
 290 oil biodiesel was above the EU standard limits and was measured to be 1.06 mg KOH/g. Finally, the
 291 cloud point and the pour point of the biodiesel was 0 and -3 °C respectively, indicating this fuel is
 292 suitable for relative cold climates.

293

294 Table 4 Physicochemical properties of the synthesised biodiesel

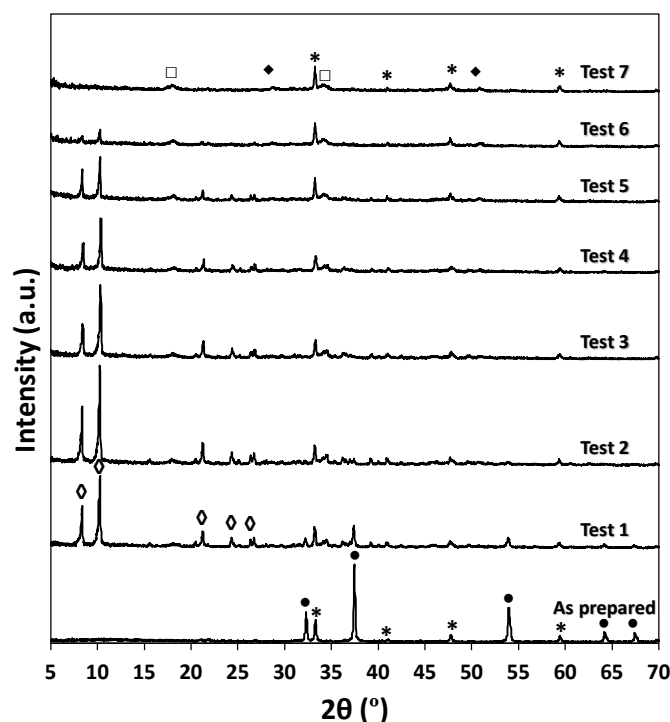
| Property | Value | EU standard limits |
|------------------------------|-----------------------|---------------------------|
| Visual observations at 15 °C | Dark orange liquid | - |
| Ester content | 97% | ≥96.5% |
| Density at 15 °C | 888 kg/m ³ | 860-900 kg/m ³ |
| Acid value | 1.06 mg KOH/g | ≤0.5 mg KOH/g |
| Cloud point | 0 °C | - |
| Pour point | -3 °C | - |
| Boiling point | 227 °C | - |

295

296 **3.5. Post-test catalyst characterisation**

297 To understand the changes in the catalyst's activity during the cycling experiments, post-test
 298 characterisation of the 6Ca/Al catalyst was performed. Figure 7 shows the room temperature XRD
 299 patterns of 6Ca/Al at the end of each test. The catalyst was recovered from the reaction mixture,
 300 washed with methanol and dried overnight at 80 °C. For comparison, the XRD pattern of the as-
 301 prepared catalyst is presented, which shows the peaks corresponding to the CaO and C3A phases,
 302 as discussed in paragraph 3.1.

303 According to the XRD analysis, the C3A phase was retained during the recycling of the catalyst over
 304 all seven tests. There were observed no changes in the peak positions or their intensities. However,
 305 after the first test, the intensities of the peaks corresponding to the CaO phase decreased significantly
 306 and an additional phase was observed. This phase was identified as calcium diglyceroxide
 307 (CaDG).[46–48] The CaDG phase gradually disappeared during the recycling of the catalyst and by
 308 the end of test 7, there was no evidence of this phase according to the XRD data. Moreover, the
 309 formation of Ca(OH)₂ and CaCO₃ progressively took place. By the end of test seven, when the catalyst
 310 was fully deactivated, the C3A phase was retained, there was no evidence of the CaDG phase and
 311 the only Ca species observed were CaCO₃ and Ca(OH)₂.



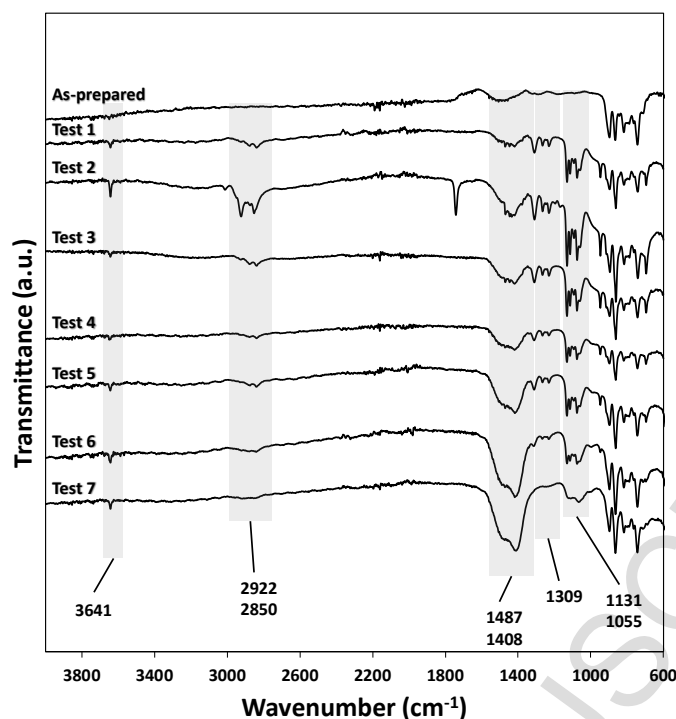
312

313 Figure 7 Phase evolution during the recyclability test of the 6Ca/Al catalyst, where (*) corresponds to the C3A
 314 phase, (●) to CaO, (◇) to CaDG, (□) to Ca(OH)₂ and (◆) to CaCO₃

315

316 Alongside the XRD analysis, FTIR spectroscopy was performed for the 6Ca/Al catalyst. Figure 8
 317 presents the evolution of the FTIR spectra of the catalyst during the progression of a series of biodiesel
 318 tests. After the first test extra transmittance bands appeared, which are characteristic of the CaDG
 319 phase.[35,46,47,49–51] More specifically, the bands at 2922 and 2850 cm⁻¹ are attributed to the C-H
 320 stretching vibration and at 1309 cm⁻¹ to the C-H bending vibration. Moreover, the band at
 321 1135 cm⁻¹ corresponds to the C-O stretching vibration in the C₂OH group and the band at 1055 cm⁻¹
 322 to the stretching vibration of C-O in the COH group of diglyceroxide. Finally, the band at 3641 cm⁻¹
 323 can be attributed to the -OH stretching vibration of the COH group of the glyceroxide bonded to the
 324 calcium atoms. However, this band can overlap with the bands that correspond to the Ca(OH)₂
 325 formation and it can be difficult to distinguish between the two contributions.

326 During the catalyst's reusability tests, it was noticed that the intensity of the transmittance bands that
 327 corresponded to the CaDG phase gradually decreased. Moreover, some transmittance bands in the
 328 region of 1408-1487 cm⁻¹ progressively appeared. These bands correspond to the formation of
 329 CaCO₃. [50,52] Therefore, when the catalyst was deactivated after test seven, the main transmittance
 330 bands that were evident were the ones in the regions of 3641 cm⁻¹ and 1408-1487 cm⁻¹, which can be
 331 attributed to the formation of Ca(OH)₂ and CaCO₃, respectively. These results were in good agreement
 332 with the XRD analysis presented in Figure 7.



333

334 Figure 8 FTIR spectra of the 6Ca/Al catalyst after each test during the recyclability test

335

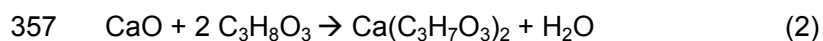
336 Furthermore, the changes in the Ca/Al ratio of the 6Ca/Al catalyst were measured by ICP-OES and
 337 EDX, before and after the reusability experiment. As presented in Table 5, the Ca/Al ratio decreased
 338 from 6 to approximately 3.5 and the two techniques demonstrated comparable results. The slightly
 339 higher Ca/Al ratios detected by EDX, suggested that the surface of the catalyst was Ca-rich. The
 340 decrease in the catalyst's Ca/Al ratio is attributed to leaching of Ca ions, and supports the data
 341 collected by XRD and IR. More specifically, since the C3A phase was stable according to XRD, the
 342 decrease in the Ca/Al ratio was due to the leaching of Ca ions from the CaO phase. Finally, the post-
 343 test Ca/Al ratio, that was approximately 3.5, was much higher than the theoretical Ca/Al ratio (1.5) of
 344 the pure C3A phase. This suggests there were still free Ca species on the surface of the catalyst.
 345 These species are most likely $\text{Ca}(\text{OH})_2$ and CaCO_3 , according to XRD and FTIR. However, these
 346 phases are much less active for the transesterification reaction and led to the deactivation of the
 347 catalyst.[35]

348 Table 5 Ca/Al ratios of the 6Ca/Al catalyst

| | as-prepared | post-test |
|---------|-------------|-----------|
| ICP-OES | 5.9 | 3.3 |
| EDX | 7.2 | 3.7 |

3.6. Reactions mechanism

349
350 Summarising the post-test characterisation performed by XRD, IR, ICP-OES and EDX the phase
351 transformations that took place during these experiments and the catalysts deactivation mechanism
352 can be explained. More specifically, the XRD data alongside the FTIR analysis were a strong indication
353 that the formation of the CaDG phase took place after the first test of the catalyst. The formation of
354 the CaDG phase during the transesterification reaction is not unusual, when CaO species are present.
355 According to the literature, CaO can react with the glycerol produced during the reaction and CaDG is
356 formed with water according to equation 2.[46,47,51]



358 The formation of the CaDG phase can enhance the catalytic activity of CaO, due to the non-protonated
359 O atoms that can be exposed on the surface of the catalyst[46,47] or it can act as an emulsifier and
360 improve the mass transfer limitations that can occur in the reaction mixture.[51] This can be confirmed
361 by the improved performance of the catalysts observed after the first test (Figure 6), when the CaDG
362 phase formed.

363 However, based on the XRD and FTIR results, the CaDG progressively disappeared during the
364 recycling of the catalyst indicating potential leaching of this phase. This can occur during the reaction
365 or during the filtration and washing of the catalyst. According to the literature, in the presence of water
366 CaDG can be hydrolysed according to equation 3.[27]



368 Therefore, when this reaction takes place it can lead to leaching of Ca^{2+} ions, as confirmed by ICP-
369 OES and EDX.

370 Finally, the disappearance of the CaDG phase was followed by the formation of $\text{Ca}(\text{OH})_2$ and CaCO_3
371 species. The formation of the $\text{Ca}(\text{OH})_2$ and CaCO_3 phases took place due to the catalyst's hydration
372 (Equation 4) and the carbonisation (Equation 5) when the catalyst was exposed to ambient air or to
373 the water produced in the reaction mixture.[27,35]



376 This led to the deactivation of the catalyst, as these species are less active for the transesterification
377 reaction than CaO.[35] However, it is worth pointing out that the hydration and carbonisation of CaO
378 took place progressively, while the decrease of the CaDG phase occurred, as it was observed by XRD
379 (Figure 7) and FTIR (Figure 8). This suggests the CaDG can form a protective layer on the surface of
380 the catalyst and hinder its deactivation due to hydration and carbonisation. Similar observations have
381 been reported in the literature by Kouzu *et al.*[46] and Endalew *et al.*[53]

382 4. Conclusions

383 In this work, the synthesis and characterisation of a series of CaO-Ca₃Al₂O₆ mixed oxides were
384 investigated as potential solid base catalysts for biodiesel production from waste fish oil. The activity
385 of the catalysts for the transesterification reaction of cod liver oil with methanol was evaluated. The
386 6Ca/Al catalyst was identified as the optimum composition in terms of catalytic activity and stability,
387 as it was reused successfully over seven consecutive tests. This catalyst was more stable than pure
388 CaO, which was reused for five tests, indicating that by incorporating the Ca₃Al₂O₆ phase, it was
389 possible to enhance the stability of the catalytically active species. Post-test characterisation of the
390 catalyst suggested that the formation of Ca diglyceroxide took place, which enhanced the reaction
391 rate. However, deactivation of the catalyst, after seven consecutive tests, occurred due to leaching of
392 Ca²⁺ ions from the active phase. Finally, the formation of Ca(OH)₂ and CaCO₃ species took place due
393 to hydration and carbonisation of the free CaO.

394 5. Acknowledgements

395 The authors would like to acknowledge Innovate UK for funding. Additionally, the authors would like
396 to thank Dr Gavin Peters for the TGA and ICP-OES measurements. Finally, we would like to thank the
397 Engineering and Physical Sciences Research Council, University of St Andrews, and CRITICAT
398 Centre for Doctoral Training for financial support [Ph.D. studentship to M.D.V.T, S.G, and E. B; Grant
399 code: EP/L016419/1].

400 6. References

- 401 [1] R. Yahyaee, B. Ghobadian, G. Najafi, Waste fish oil biodiesel as a source of renewable fuel in Iran,
402 *Renew. Sustain. Energy Rev.* 17 (2013) 312–319. doi:10.1016/j.rser.2012.09.025.
- 403 [2] J.F.X. Silva, K. Ribeiro, J.F. Silva, T.B. Cahú, R.S. Bezerra, Utilization of tilapia processing waste
404 for the production of fish protein hydrolysate, *Anim. Feed Sci. Technol.* 196 (2014) 96–106.
405 doi:10.1016/j.anifeedsci.2014.06.010.
- 406 [3] P.J. García-Moreno, M. Khanum, A. Guadix, E.M. Guadix, Optimization of biodiesel production from
407 waste fish oil, *Renew. Energy.* 68 (2014) 618–624. doi:10.1016/j.renene.2014.03.014.
- 408 [4] B. Jamilah, K.G. Harvinder, Properties of gelatins from skins of fish - Black tilapia (*Oreochromis*
409 *mossambicus*) and red tilapia (*Oreochromis nilotica*), *Food Chem.* 77 (2002) 81–84.
410 doi:10.1016/S0308-8146(01)00328-4.
- 411 [5] D. Madhu, B. Singh, Y.C. Sharma, Studies on application of fish waste for synthesis of high quality
412 biodiesel, *RSC Adv.* 4 (2014) 31462–31468. doi:10.1039/C4RA03590A.
- 413 [6] K. Jayathilakan, K. Sultana, K. Radhakrishna, A.S. Bawa, Utilization of byproducts and waste
414 materials from meat, poultry and fish processing industries: A review, *J. Food Sci. Technol.* 49

- 415 (2012) 278–293. doi:10.1007/s13197-011-0290-7.
- 416 [7] F. Ma, M.A. Hanna, Biodiesel production: A review, *Bioresour. Technol.* 70 (1999) 1–15.
417 doi:10.1016/S0960-8524(99)00025-5.
- 418 [8] D.Y.C. Leung, X. Wu, M.K.H. Leung, A review on biodiesel production using catalyzed
419 transesterification, *Appl. Energy*. 87 (2010) 1083–1095. doi:10.1016/j.apenergy.2009.10.006.
- 420 [9] A.E. Atabani, A.S. Silitonga, I.A. Badruddin, T.M.I. Mahlia, H.H. Masjuki, S. Mekhilef, A
421 comprehensive review on biodiesel as an alternative energy resource and its characteristics,
422 *Renew. Sustain. Energy Rev.* 16 (2012) 2070–2093. doi:10.1016/j.rser.2012.01.003.
- 423 [10] A.F. Lee, J.A. Bennett, J.C. Manayil, K. Wilson, Heterogeneous catalysis for sustainable biodiesel
424 production *via* esterification and transesterification, *Chem. Soc. Rev.* 43 (2014) 7887–7916.
425 doi:10.1039/C4CS00189C.
- 426 [11] G. Knothe, L.F. Razon, Biodiesel fuels, *Prog. Energy Combust. Sci.* 58 (2017) 36–59.
427 doi:10.1016/j.pecs.2016.08.001.
- 428 [12] G. Knothe, Biodiesel and renewable diesel: A comparison, *Prog. Energy Combust. Sci.* 36 (2010)
429 364–373. doi:10.1016/j.pecs.2009.11.004.
- 430 [13] L.C. Meher, D. Vidya Sagar, S.N. Naik, Technical aspects of biodiesel production by
431 transesterification - A review, *Renew. Sustain. Energy Rev.* 10 (2006) 248–268.
432 doi:10.1016/j.rser.2004.09.002.
- 433 [14] L.T. Thanh, K. Okitsu, L. Van Boi, Y. Maeda, Catalytic Technologies for Biodiesel Fuel Production
434 and Utilization of Glycerol: A Review, *Catalysts*. 2 (2012) 191–222. doi:10.3390/catal2010191.
- 435 [15] I.M. Atadashi, M.K. Aroua, A.R. Abdul Aziz, N.M.N. Sulaiman, The effects of catalysts in biodiesel
436 production: A review, *J. Ind. Eng. Chem.* 19 (2013) 14–26. doi:10.1016/j.jiec.2012.07.009.
- 437 [16] A.N. Phan, A.P. Harvey, V. Eze, Rapid Production of Biodiesel in Mesoscale Oscillatory Baffled
438 Reactors, *Chem. Eng. Technol.* 35 (2012) 1214–1220. doi:10.1002/ceat.201200031.
- 439 [17] V.C. Eze, A.N. Phan, C. Pirez, A.P. Harvey, A.F. Lee, K. Wilson, Heterogeneous catalysis in an
440 oscillatory baffled flow reactor, *Catal. Sci. Technol.* 3 (2013) 2373. doi:10.1039/c3cy00282a.
- 441 [18] Z. Qiu, L. Zhao, L. Weatherley, Process intensification technologies in continuous biodiesel
442 production, *Chem. Eng. Process. Process Intensif.* 49 (2010) 323–330.
443 doi:10.1016/j.cep.2010.03.005.
- 444 [19] J.S. Lee, S. Saka, Biodiesel production by heterogeneous catalysts and supercritical technologies,
445 *Bioresour. Technol.* 101 (2010) 7191–7200. doi:10.1016/j.biortech.2010.04.071.
- 446 [20] D. Madhu, R. Arora, S. Sahani, V. Singh, Y.C. Sharma, Synthesis of High-Quality Biodiesel Using

- 447 Feedstock and Catalyst Derived from Fish Wastes, *J. Agric. Food Chem.* 65 (2017) 2100–2109.
448 doi:10.1021/acs.jafc.6b05608.
- 449 [21] B. Salamatina, A.Z. Abdullah, S. Bhatia, Quality evaluation of biodiesel produced through
450 ultrasound-assisted heterogeneous catalytic system, *Fuel Process. Technol.* 97 (2012) 1–8.
451 doi:10.1016/j.fuproc.2012.01.003.
- 452 [22] B. Sajjadi, A.R.A. Aziz, S. Ibrahim, Investigation , modelling and reviewing the effective parameters
453 in microwave-assisted transesterification, *Renew. Sustain. Energy Rev.* 37 (2014) 762–777.
454 doi:10.1016/j.rser.2014.05.021.
- 455 [23] W. Xu, L. Gao, S. Wang, G. Xiao, Biodiesel production in a membrane reactor using MCM-41
456 supported solid acid catalyst, *Bioresour. Technol.* 159 (2014) 286–291.
457 doi:10.1016/j.biortech.2014.03.004.
- 458 [24] N. nan Boon-anuwat, W. Kiatkittipong, F. Aiouache, S. Assabumrungrat, Process design of
459 continuous biodiesel production by reactive distillation: Comparison between homogeneous and
460 heterogeneous catalysts, *Chem. Eng. Process. Process Intensif.* 92 (2015) 33–44.
461 doi:10.1016/j.cep.2015.03.025.
- 462 [25] L.P. Christopher, Hemanathan Kumar, V.P. Zambare, Enzymatic biodiesel: Challenges and
463 opportunities, *Appl. Energy.* 119 (2014) 497–520. doi:10.1016/j.apenergy.2014.01.017.
- 464 [26] A.P.S. Chouhan, A.K. Sarma, Modern heterogeneous catalysts for biodiesel production: A
465 comprehensive review, *Renew. Sustain. Energy Rev.* 15 (2011) 4378–4399.
466 doi:10.1016/j.rser.2011.07.112.
- 467 [27] N. Oueda, Y.L. Bonzi-Coulibaly, I.W.K. Ouédraogo, Deactivation Processes, Regeneration
468 Conditions and Reusability Performance of CaO or MgO Based Catalysts Used for Biodiesel
469 Production—A Review, *Mater. Sci. Appl.* 08 (2017) 94–122. doi:10.4236/msa.2017.81007.
- 470 [28] C.S. MacLeod, A.P. Harvey, A.F. Lee, K. Wilson, Evaluation of the activity and stability of alkali-
471 doped metal oxide catalysts for application to an intensified method of biodiesel production, *Chem.*
472 *Eng. J.* 135 (2008) 63–70. doi:10.1016/j.cej.2007.04.014.
- 473 [29] S. Benjapornkulaphong, C. Ngamcharussrivichai, K. Bunyakiat, Al₂O₃-supported alkali and alkali
474 earth metal oxides for transesterification of palm kernel oil and coconut oil, *Chem. Eng. J.* 145 (2009)
475 468–474. doi:10.1016/j.cej.2008.04.036.
- 476 [30] M. Zabeti, W.M.A.W. Daud, M.K. Aroua, Biodiesel production using alumina-supported calcium
477 oxide: An optimization study, *Fuel Process. Technol.* 91 (2010) 243–248.
478 doi:10.1016/j.fuproc.2009.10.004.
- 479 [31] J. Chen, L. Jia, X. Guo, L. Xiang, S. Lou, Production of novel biodiesel from transesterification over
480 KF-modified Ca–Al hydrotalcite catalyst, *RSC Adv.* 4 (2014) 60025–60033.

- 481 doi:10.1039/C4RA09214G.
- 482 [32] M. Di Serio, M. Ledda, M. Cozzolino, G. Minutillo, R. Tesser, E. Santacesaria, Transesterification of
483 Soybean oil to biodiesel by using heterogeneous basic catalysts., *Ind. Eng. Chem. Res.* 45 (2006)
484 3009–14.
- 485 [33] J.J. Woodford, C.M.A. Parlett, J. Dacquin, G. Cibin, A. Dent, J. Montero, A.F. Lee, Identifying the
486 active phase in Cs-promoted MgO nanocatalysts for triglyceride transesterification, *J Chem Technol*
487 *Biotechnol.* 89 (2014) 73–80. doi:10.1002/jctb.4098.
- 488 [34] D.M. Marinković, M. V. Stanković, A. V. Veličković, J.M. Avramović, M.R. Miladinović, O.O.
489 Stamenković, V.B. Veljković, D.M. Jovanović, Calcium oxide as a promising heterogeneous catalyst
490 for biodiesel production: Current state and perspectives, *Renew. Sustain. Energy Rev.* 56 (2016)
491 1387–1408. doi:10.1016/j.rser.2015.12.007.
- 492 [35] M. Kouzu, T. Kasuno, M. Tajika, Y. Sugimoto, S. Yamanaka, J. Hidaka, Calcium oxide as a solid
493 base catalyst for transesterification of soybean oil and its application to biodiesel production, *Fuel.*
494 87 (2008) 2798–2806. doi:10.1016/j.fuel.2007.10.019.
- 495 [36] Z. Kesic, I. Lukic, M. Zdujic, L. Mojovic, D. Skala, Calcium oxide based catalysts for biodiesel
496 production: A review, *Chem. Ind. Chem. Eng. Q.* 22 (2016) 391–408.
497 doi:10.2298/CICEQ160203010K.
- 498 [37] A. Molaei Dehkordi, M. Ghasemi, Transesterification of waste cooking oil to biodiesel using Ca and
499 Zr mixed oxides as heterogeneous base catalysts, *Fuel Process. Technol.* 97 (2012) 45–51.
500 doi:10.1016/j.fuproc.2012.01.010.
- 501 [38] M. Kim, C. DiMaggio, S. Yan, S.O. Salley, K.Y.S. Ng, The effect of support material on the
502 transesterification activity of CaO–La₂O₃ and CaO–CeO₂ supported catalysts, *Green Chem.* 13
503 (2011) 334–339. doi:10.1039/C0GC00828A.
- 504 [39] B. Wang, S. Li, S. Tian, R. Feng, Y. Meng, A new solid base catalyst for the transesterification of
505 rapeseed oil to biodiesel with methanol, *Fuel.* 104 (2013) 698–703. doi:10.1016/j.fuel.2012.08.034.
- 506 [40] Y.L. Meng, B.Y. Wang, S.F. Li, S.J. Tian, M.H. Zhang, Effect of calcination temperature on the
507 activity of solid Ca/Al composite oxide-based alkaline catalyst for biodiesel production, *Bioresour.*
508 *Technol.* 128 (2013) 305–309. doi:10.1016/j.biortech.2012.10.152.
- 509 [41] G. Knothe, Monitoring a progressing transesterification reaction by fiber-optic near infrared
510 spectroscopy with correlation to ¹H nuclear magnetic resonance spectroscopy, *JAOCS, J. Am. Oil*
511 *Chem. Soc.* 77 (2000) 489–493. doi:10.1007/s11746-000-0078-5.
- 512 [42] S. Yan, H. Lu, B. Liang, Supported CaO Catalysts Used in the Transesterification of Rapeseed Oil
513 for the Purpose of Biodiesel Production Supported CaO Catalysts Used in the Transesterification of
514 Rapeseed Oil for the Purpose of Biodiesel Production, *Energy & Fuels.* (2008) 1–7.

- 515 doi:10.1021/ef070105o.
- 516 [43] M.C.G. Albuquerque, I. Jiménez-Urbistondo, J. Santamaría-González, J.M. Mérida-Robles, R.
517 Moreno-Tost, E. Rodríguez-Castellón, A. Jiménez-López, D.C.S. Azevedo, C.L. Cavalcante, P.
518 Maireles-Torres, CaO supported on mesoporous silicas as basic catalysts for transesterification
519 reactions, *Appl. Catal. A Gen.* 334 (2008) 35–43. doi:10.1016/j.apcata.2007.09.028.
- 520 [44] H. V Lee, J.C. Juan, N.F. Binti Abdullah, R. Nizah Mf, Y.H. Taufiq-Yap, Heterogeneous base
521 catalysts for edible palm and non- edible *Jatropha*- based biodiesel production, *Chem. Cent. J.* 8
522 (2014) 1–9. doi:10.1186/1752-153X-8-30.
- 523 [45] M. Kouzu, J.S. Hidaka, Transesterification of vegetable oil into biodiesel catalyzed by CaO: A
524 review, *Fuel.* 93 (2012) 1–12. doi:10.1016/j.fuel.2011.09.015.
- 525 [46] M. Kouzu, T. Kasuno, M. Tajika, S. Yamanaka, J. Hidaka, Active phase of calcium oxide used as
526 solid base catalyst for transesterification of soybean oil with refluxing methanol, *Appl. Catal. A Gen.*
527 334 (2008) 357–365. doi:10.1016/j.apcata.2007.10.023.
- 528 [47] L. León-Reina, A. Cabeza, J. Rius, P. Maireles-Torres, A.C. Alba-Rubio, M. López Granados,
529 Structural and surface study of calcium glyceroxide, an active phase for biodiesel production under
530 heterogeneous catalysis, *J. Catal.* 300 (2013) 30–36. doi:10.1016/j.jcat.2012.12.016.
- 531 [48] M. Kouzu, S. ya Yamanaka, J. suke Hidaka, M. Tsunomori, Heterogeneous catalysis of calcium
532 oxide used for transesterification of soybean oil with refluxing methanol, *Appl. Catal. A Gen.* 355
533 (2009) 94–99. doi:10.1016/j.apcata.2008.12.003.
- 534 [49] W. Huang, S. Tang, H. Zhao, S. Tian, Activation of commercial CaO for biodiesel production from
535 rapeseed oil using a novel deep eutectic solvent, *Ind. Eng. Chem. Res.* 52 (2013) 11943–11947.
536 doi:10.1021/ie401292w.
- 537 [50] F.S.H. Simanjuntak, T.K. Kim, S.D. Lee, B.S. Ahn, H.S. Kim, H. Lee, CaO-catalyzed synthesis of
538 glycerol carbonate from glycerol and dimethyl carbonate: Isolation and characterization of an active
539 Ca species, *Appl. Catal. A Gen.* 401 (2011) 220–225. doi:10.1016/j.apcata.2011.05.024.
- 540 [51] I. Lukić, Ž. Kesić, M. Zdujić, D. Skala, Calcium diglyceroxide synthesized by mechanochemical
541 treatment, its characterization and application as catalyst for fatty acid methyl esters production,
542 *Fuel.* 165 (2016) 159–165. doi:10.1016/j.fuel.2015.10.063.
- 543 [52] W. Xie, L. Zhao, Production of biodiesel by transesterification of soybean oil using calcium supported
544 tin oxides as heterogeneous catalysts, *Energy Convers. Manag.* 76 (2013) 55–62.
545 doi:10.1016/j.enconman.2013.07.027.
- 546 [53] A.K. Endalew, Y. Kiros, R. Zanzi, Heterogeneous catalysis for biodiesel production from *Jatropha*
547 *curcas* oil (JCO) Heterogeneous catalysis for biodiesel production from *Jatropha curcas* oil (JCO
548), *Energy.* 36 (2011) 2693–2700. doi:10.1016/j.energy.2011.02.010.

Highlights

- Investigation of the CaO-Ca₃Al₂O₆ catalyst for biodiesel synthesis from fish oil
- The optimum ratio in terms of catalytic activity and recyclability was 6Ca/Al
- The formation of an intermediate, more active phase was identified by XRD and IR
- 6Ca/Al catalyst was recycled successfully for 7 consecutive cycles